Supporting Information

Two-dimensional graphene-directed formation of the cylindrical iron nanocapsules for Fischer-Tropsch synthesis

*Feng Jiang, Bing Liu,Weiping Li, Min Zhang, Zaijun Li, and Xiaohao Liu**

Department of Chemical Engineering, School of Chemical and Material Engineering, Jiangnan University, Wuxi 214122, China
E-mail: liuxh@jiangnan.edu.cn (X.H. Liu)

Contents:

Supplementary Figures and Tables

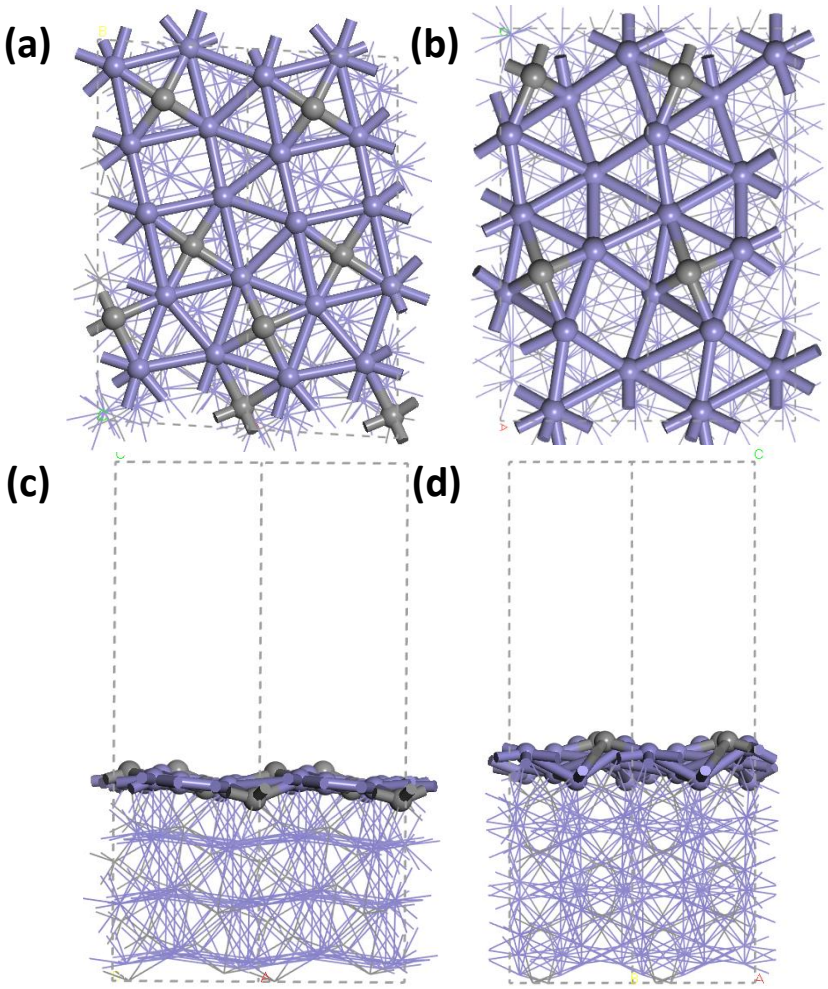

Fig. S1. Top views of (a) χ-Fe_5C_2 (510) and (b) χ-Fe_5C_2 (-202) surfaces, and side views of (c) χ-Fe_5C_2 (510) and (d) χ-Fe_5C_2 (-202) surfaces (blue: Fe atoms; grey: C atoms).

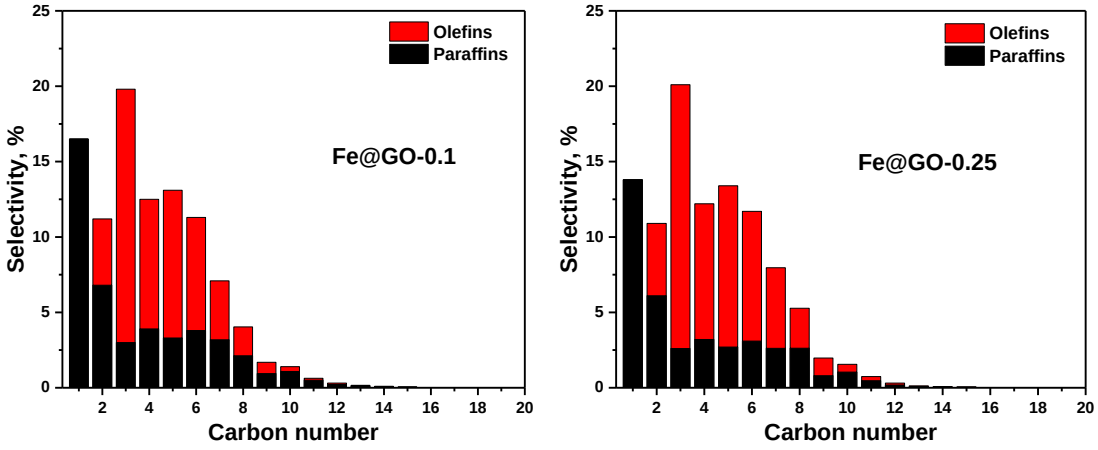

Fig. S2. The product distribution obtained over GO modified Fe_2O_3 catalysts after 50 h reaction. The selectivities to higher olefins (total olefins) for Fe@GO-0.1 and Fe@GO-0.25 catalysts are 24.5% (54.4%), and 29.5% (60.7%), respectively. Reaction conditions: catalyst = 0.1 g, H_2/CO = 1.0, GHSV = 22.2 L $g_{cat}^{-1}h^{-1}$, 340 ℃, 1.0 MPa, 50 h.

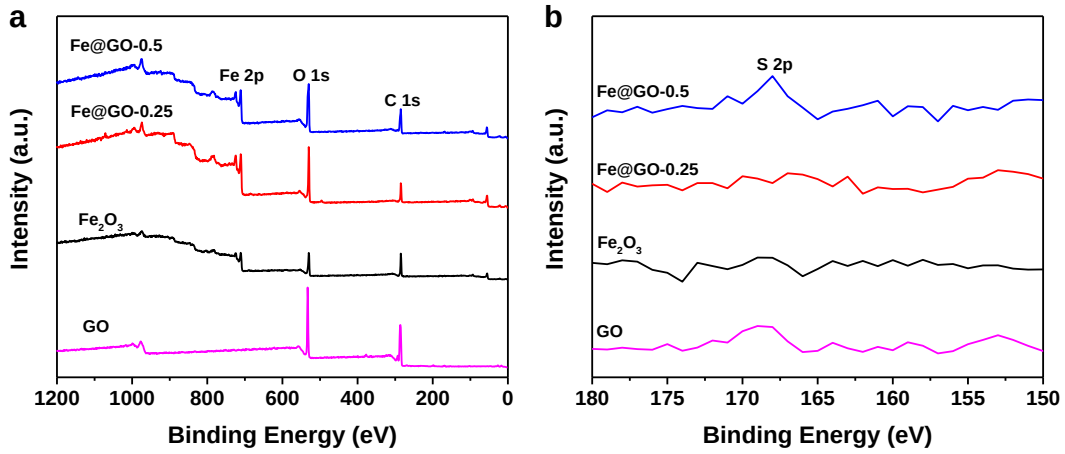

Fig. S3. The XPS spectra of fresh GO and Fe@GO catalysts: a) the full spectra, b) the S 2p spectra.

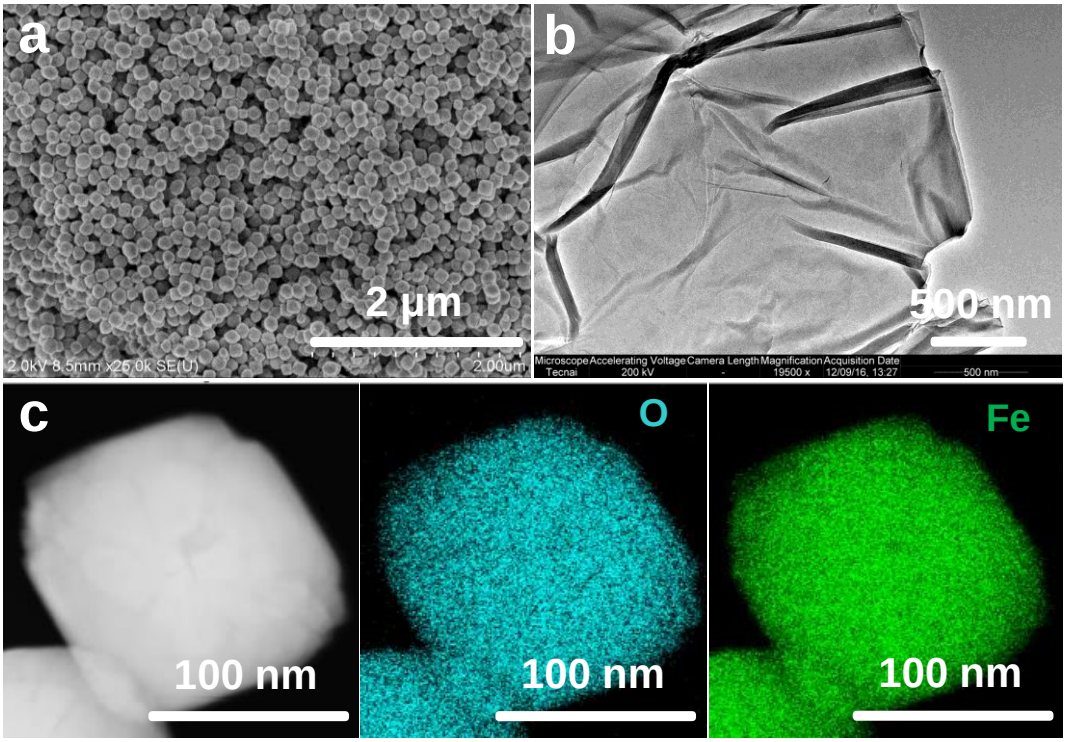

Fig. S4. (a) SEM image of Fe_2O_3 NPs, (b) TEM image of GO, and (c) original STEM image of Fe_2O_3 NPs and corresponding STEM-EDX elemental mapping of Fe and O on the Fe_2O_3 NPs.

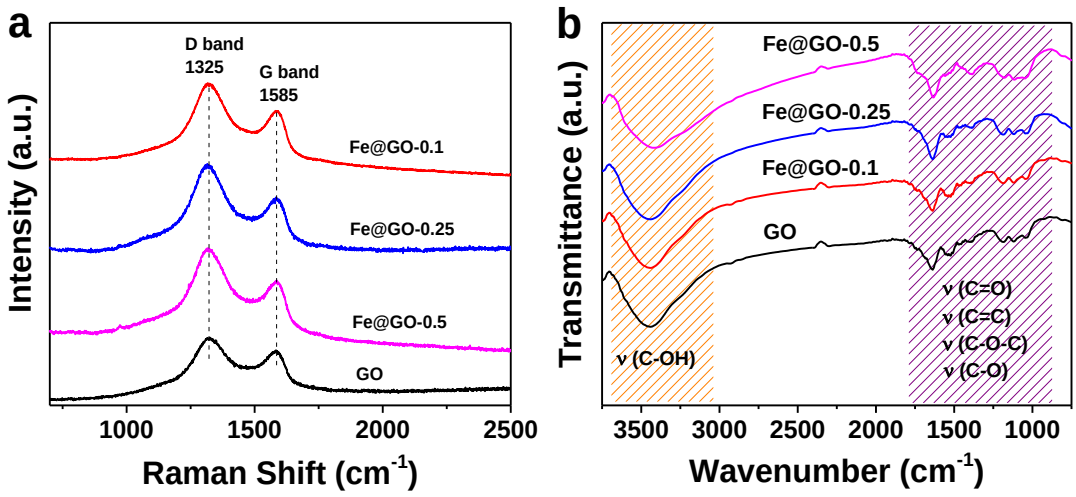

Fig. S5. (a) Raman spectra of GO and GO modified Fe_2O_3 catalysts; (b) FTIR spectra of GO and GO modified Fe_2O_3 catalysts.

Raman spectra of GO and Fe@GO catalysts exhibit two distinct peaks due to the D and G bands at around 1325 and 1585 cm^{-1}, respectively.[1] The D band is attributed to an A_{1g} vibration mode of carbon atoms with a double-resonance process in plane terminations of disordered graphite. The G band arises from the E_{2g} mode of graphitic carbon and is assigned to the vibration of sp^2 hybridized carbon atoms in the graphite layer. The relative integrated intensity of these two bands (I_D/I_G) is usually employed as a measure of the disorder in carbon materials.[2] In our study, the I_D/I_G ratio of GO is 1.16 while no significant change in the ratio can be observed over the Fe@GO catalysts, and also no discernible Raman shift for these bands, indicating the similar nature of GO in these catalysts. The FTIR spectra of GO and Fe@GO catalysts show the vibrations of hydroxyls with contributions from COOH and H_2O (C-OH, 3000-3700 cm^{-1}) and the vibrations of other groups including C=O, C=C, C-O-C and C-O with wavenumber ranging from 1750 to 800 cm^{-1}.[3] As expected, there is negligible change in the peak intensity and peak position over the Fe@GO catalysts. In summary, the nature of GO in the Fe@GO catalysts is similar as the fresh GO.

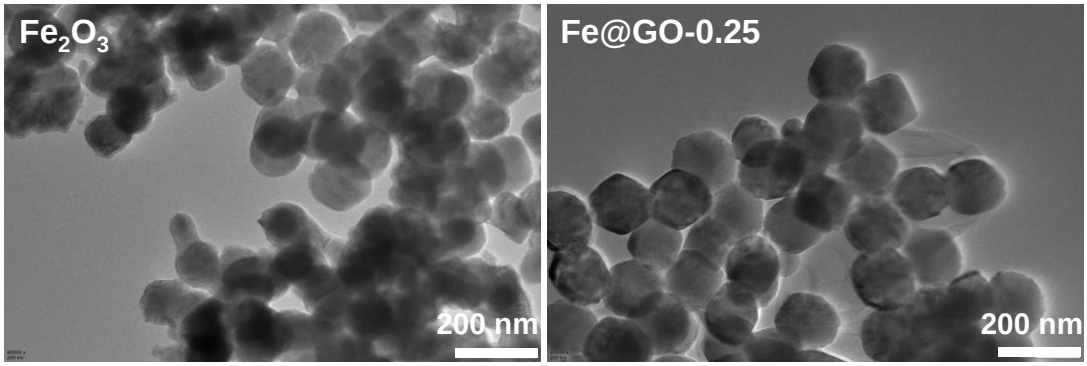

Fig. S6. TEM images of the reduced Fe_2O_3 and Fe@GO-0.25 catalysts.

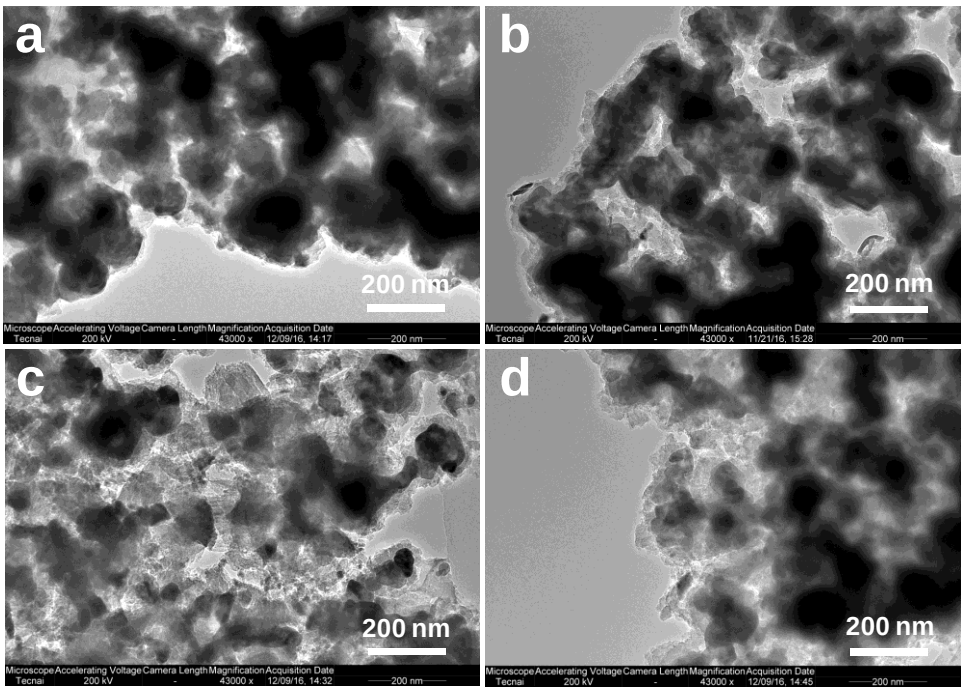

Fig. S7. TEM images of catalyst after reaction for 50 h. (a) Fe_2O_3 NPs (300 ℃), (b) Fe_2O_3 NPs (340 ℃), (c) Fe@PAA-0.25 (340 ℃), (d) Fe@PVP-0.25 (340 ℃). Reaction conditions: catalyst = 0.1 g, H_2/CO = 1.0, GHSV = 22.2 L $g_{cat}^{-1}h^{-1}$, 1.0 MPa.

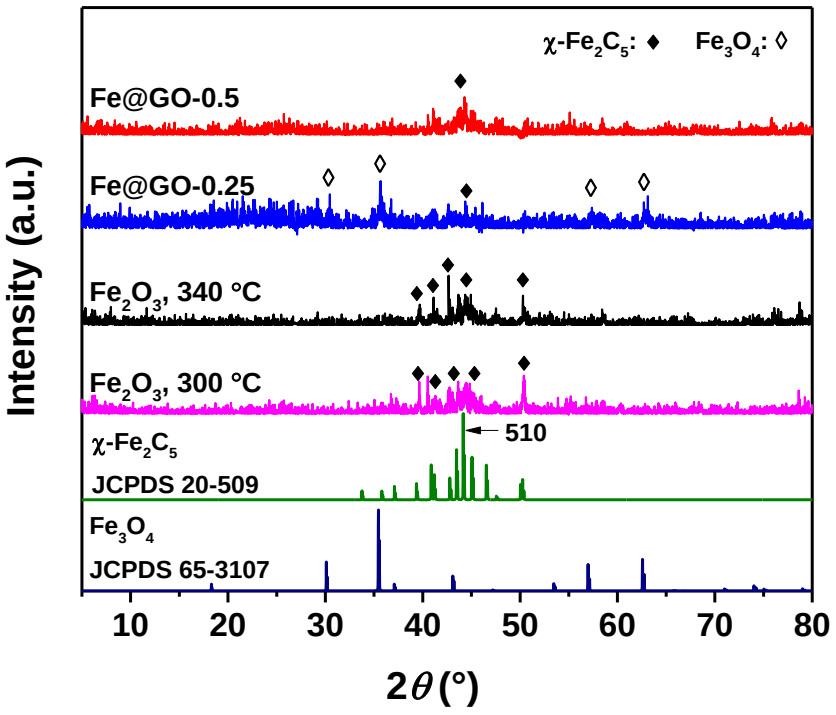

Fig. S8. XRD patterns of spent Fe_2O_3 and Fe@GO catalysts.

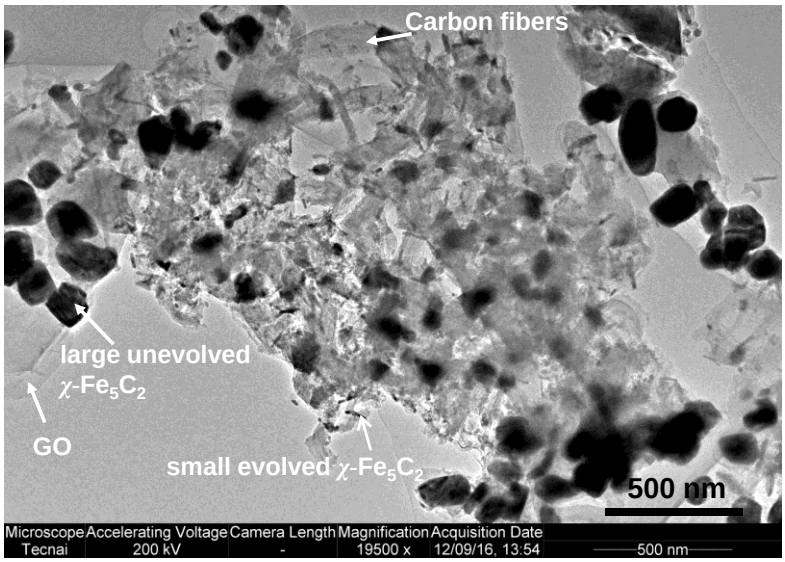

Fig. S9. TEM image of Fe@GO-0.5 catalyst after 50 h reaction.

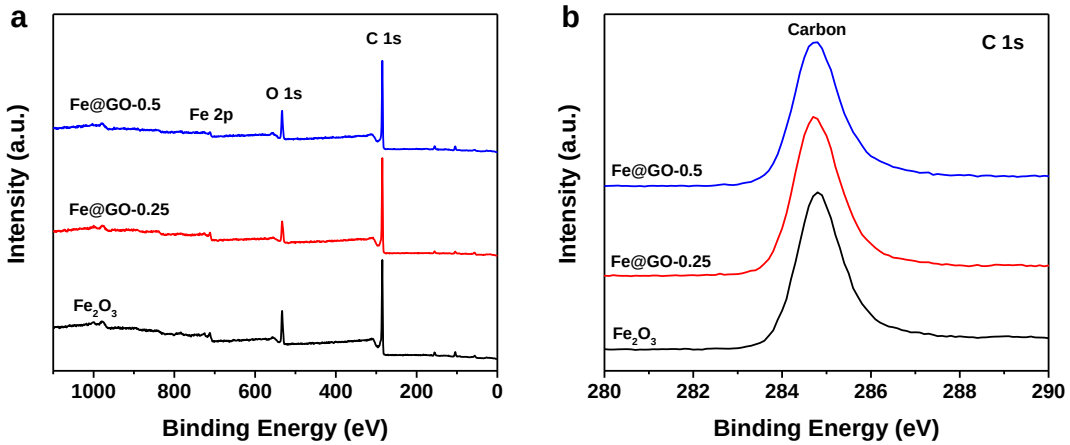

Fig. S10. The XPS spectra of spent Fe_2O_3 and Fe@GO catalysts: a) survey spectra, b) C 1s spectra.

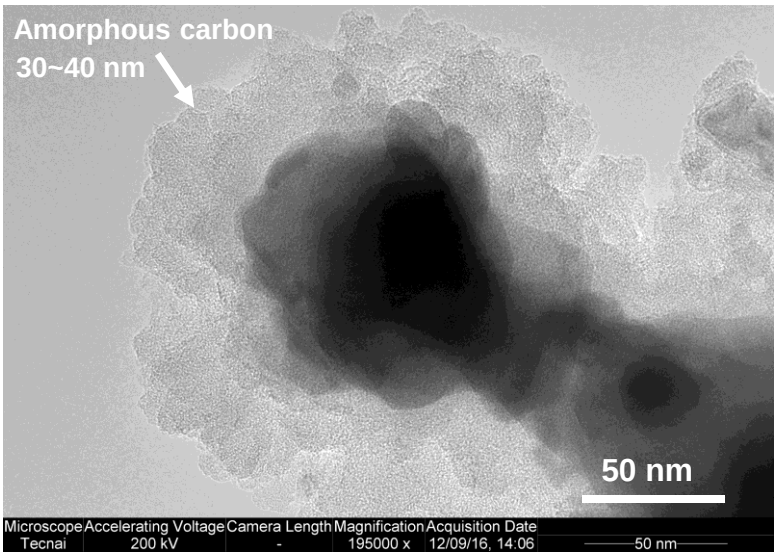

Fig. S11. TEM image of spent Fe_2O_3 (340 ℃) catalyst. Reaction conditions: catalyst = 0.1 g, H_2/CO = 1.0, GHSV = 22.2 L $g_{cat}^{-1}h^{-1}$, 1.0 MPa.

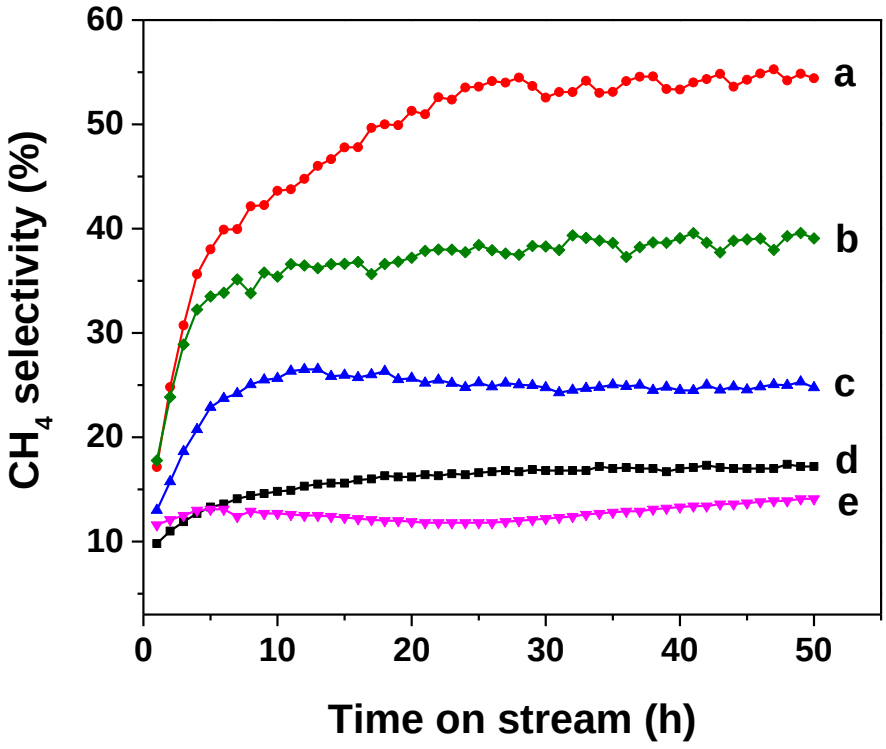

Fig. S12. Time on steam evolution of methane selectivity over unmodified and modified Fe_2O_3 catalysts. (a) Fe_2O_3 NPs (340 ℃), (b) Fe@PAA-0.25 (340 ℃), (c) Fe@PVP-0.25 (340 ℃), (d) Fe_2O_3 NPs (300 ℃) and (e) Fe@GO-0.25 (340 ℃). Reaction conditions: catalyst = 0.1 g, H_2/CO = 1.0, GHSV = 22.2 L $g_{cat}^{-1}h^{-1}$, 1.0 MPa.

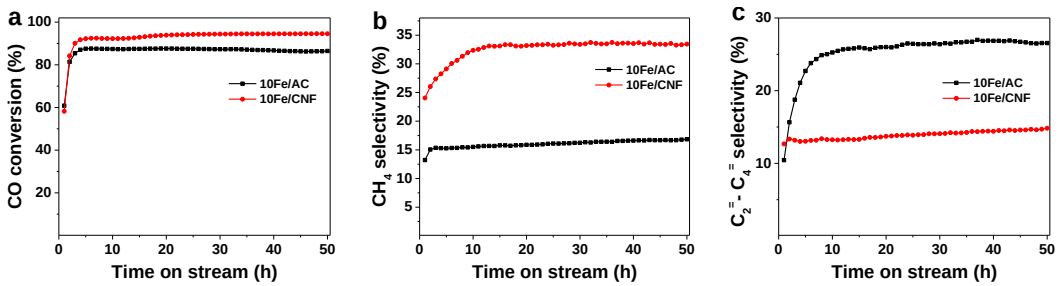

Fig. S13. Catalytic performance of different carbon material supported and sulfur promoted catalysts. (a-c) Time on stream evolution of CO conversion, methane selectivity and lower olefins selectivity over AC and CNF supported iron catalysts.

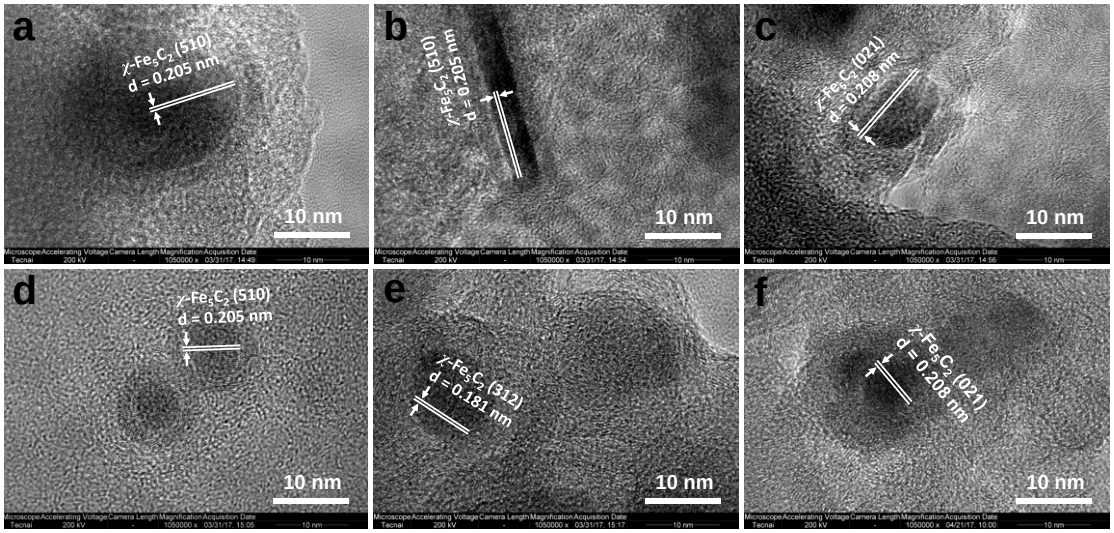

Fig. S14. HRTEM images of spent (a-c) 10Fe/AC and (d-f) 10Fe/CNF catalysts.

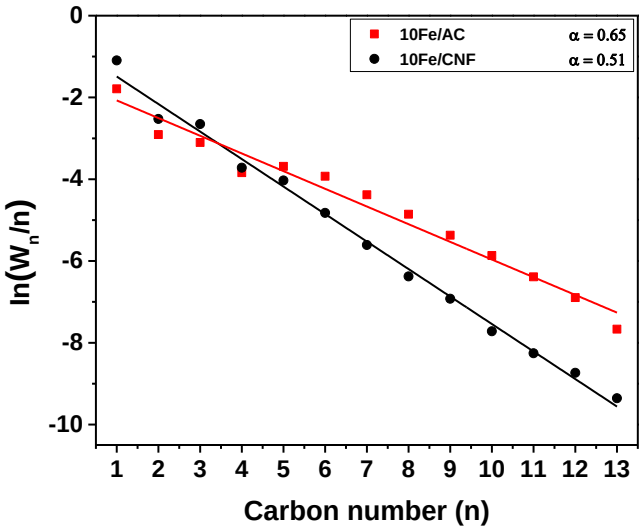

Fig. S15. ASF plots of FT products obtained over the AC and CNF supported iron catalysts.

Table S1. Elemental analysis of different carbon materials

Carbon sources	C, wt%	H, wt%	N, wt%	S, wt%
GO (fresh)	49.2	2.7	0	1.0
GO (treated)	49.0	2.5	0	0.4
PAA	49.8	6.6	0	0
PVP	60.1	8.9	11.7	0

Table S2. Comparision of the calculated lattice parameters and the average magnetic moment per iron atom obtained in this work with previous theoretical values

Method	a(Å)	b(Å)	c(Å)	β(deg)	Magnetic moment(μ_B)	ref
PAW-PBE	11.580	4.508	4.994	96.64	1.73	4
PAW-PBE	11.554	4.502	4.985	97.62	1.73	5
PAW-PBE	11.545	4.496	4.982	97.60	1.73	6
PAW-PBE	11.527	4.504	4.987	97.68	1.735	This work

Table S3. Elemental analysis of different fresh samples by XPS

	Fe_2O_3	GO	Fe@GO-0.25	Fe@GO-0.5
Fe, atomic %	10.47	0	20.04	12.37
C, atomic %	59.03	65.83	36.83	44.67
O, atomic %	30.51	32.01	43.14	42.08
K, atomic %	0	1.54	0	0.52
S, atomic %	0	0.62	0	0.36
Mn, atomic %	0	0	0	0

Table S4. Elemental analysis of different spent samples by XPS

	Fe_2O_3	Fe@GO-0.25	Fe@GO-0.5
Fe, atomic %	2.46	2.36	1.70
C, atomic %	80.76	84.4	81.52
O, atomic %	16.78	13.24	16.78
K, atomic %	0	0	0
S, atomic %	0	0	0
Mn, atomic %	0	0	0

References

1 B.F. Machado and P. Serp, *Catal. Sci. Technol*., 2012, **2**, 54-75.

2 H. Wang, J.T. Robinson, X. Li and H. Dai, *J. Am. Chem. Soc*., 2009, **131**, 9910-9911.

3 M. Acik, G. Lee, C. Mattevi, A. Pirkle, R.M. Wallace, M. Chhowalla, K. Cho and Y. Chabal, *J. Phys. Chem. C*, 2011, **115**, 19761-19781.

4 D.C. Sorescu, *J. Phys. Chem. C*, 2009, **113**, 9256-9274.

5 T.H. Pham, X.Z. Duan, G. Qian, X.G. Zhou and D. Chen, *J. Phys. Chem. C*, 2014, **118**, 10170-10176.

6 S. Zhao, X.W. Liu, C.F. Huo, Y.W. Li, J.G. Wang and H.J. Jiao, *J. Catal.*, 2012, **294**, 47-53.